Supplementary Information

Development of Portable Mobility Spectrometer for Aerosol Exposure Measurement

Pramod Kulkarni*[1], Chaolong Qi[1], Nobuhiko Fukushima[2]

[1]Centers for Disease Control and Prevention,

National Institute for Occupational Safety and Health

Cincinnati, OH, 45226

[2]Kanomax Japan Inc.

Osaka, Japan

Aerosol Science and Technology

Table S1: Centroid channel/bin diameters for EMS and PAMS used in this study at high resolution (HR) and low resolution (LR)

HR		LR	
EMS	**PAMS**	**EMS**	**PAMS**
-	10.6	-	15.1
-	11.7	-	16.4
-	12.6	20.5	20.7
14.6	14.3	24.4	30
16.6	17.3	31.6	38.4
18.8	20.3	41.5	52.3
21.4	23.3	54.8	70.5
24.5	25.9	72.7	94.3
27.8	30.1	96.7	129.2
31.8	34.8	131.2	179.5
36.3	40.2	181.8	254.9
41.6	46.3	258.1	371.3
47.3	53.3	376.5	556.5
54.7	60.7	564.1	855
62.3	70.4	871.5	-
72.3	81.5	-	-
83	94.6	-	-
95.8	110	-	-
110.8	128.3	-	-
129.2	150.3	-	-
152.6	176.9	-	-
177.8	209.2	-	-
210.5	248.8	-	-
251.2	298	-	-
299.1	359.1	-	-
363.5	435.7	-	-
438.9		-	-

Table S2: Instruments used in inter-comparison study

Model, Manufacturer	Abbreviation	Calibrated on	Type of charger, and age	Aerosol-to-sheath flow ratio
Scanning Mobility Particle Sizer * Model 3936, TSI Inc.	SMPS3936	08/2013	Bipolar, Soft X-Ray, Model 3087, TSI 07/2012	8:1
Scanning Mobility Particle Sizer, Model 3034, TSI Inc.	SMPS3034	07/2003	Bipolar, Soft X-Ray, Model 3087, TSI 06/2012	8:1
Wide Range Particle Spectrometer, Model M1000XP, MSP Inc.	WPS	12/2011	Bipolar, Po210, manufacturing date 9/2011	10:1
NanoScan SMPS Nanoparticle Sizer, Model 3910, TSI Inc.	NanoScan	04/2013	Unipolar charger	3:1
Prototype PAMS	PAMS	07/22/2014	Bipolar, Dual-Corona Ionizer	8:1 or 4:1

* The EMS instrument used in this study employed the charger, DMA, and the CPC from this SMPS3936 system

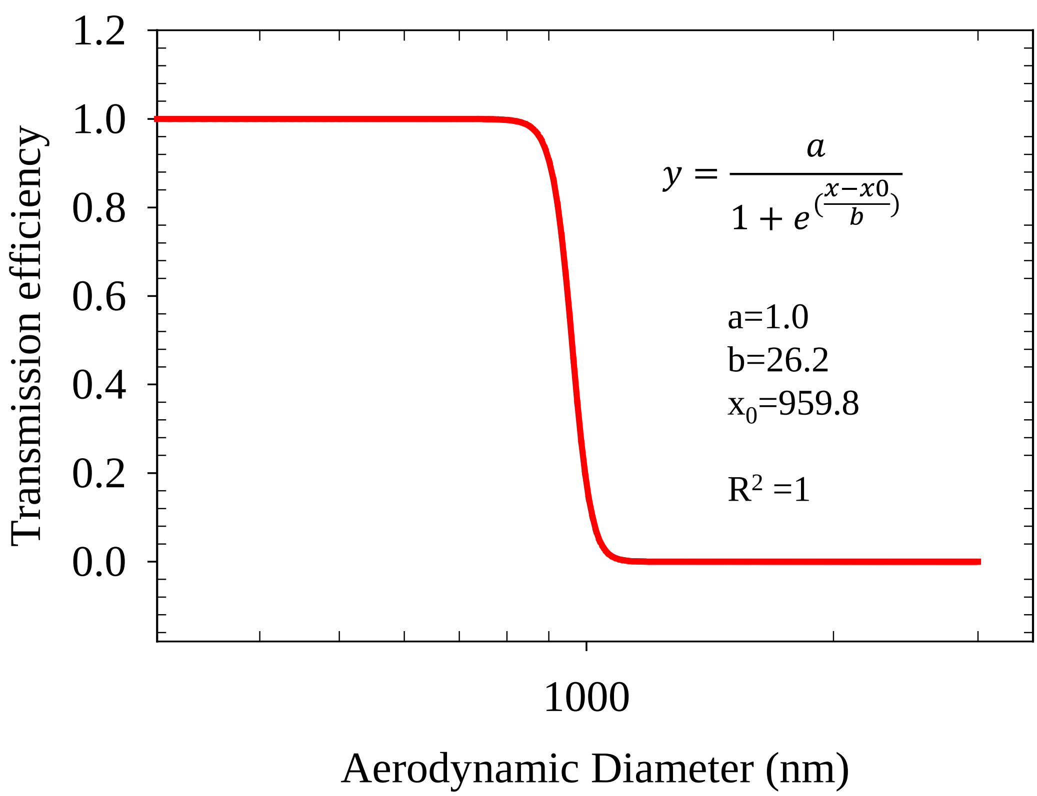

Figure S1: Transmission efficiency curve used for the inlet cyclone in PAMS

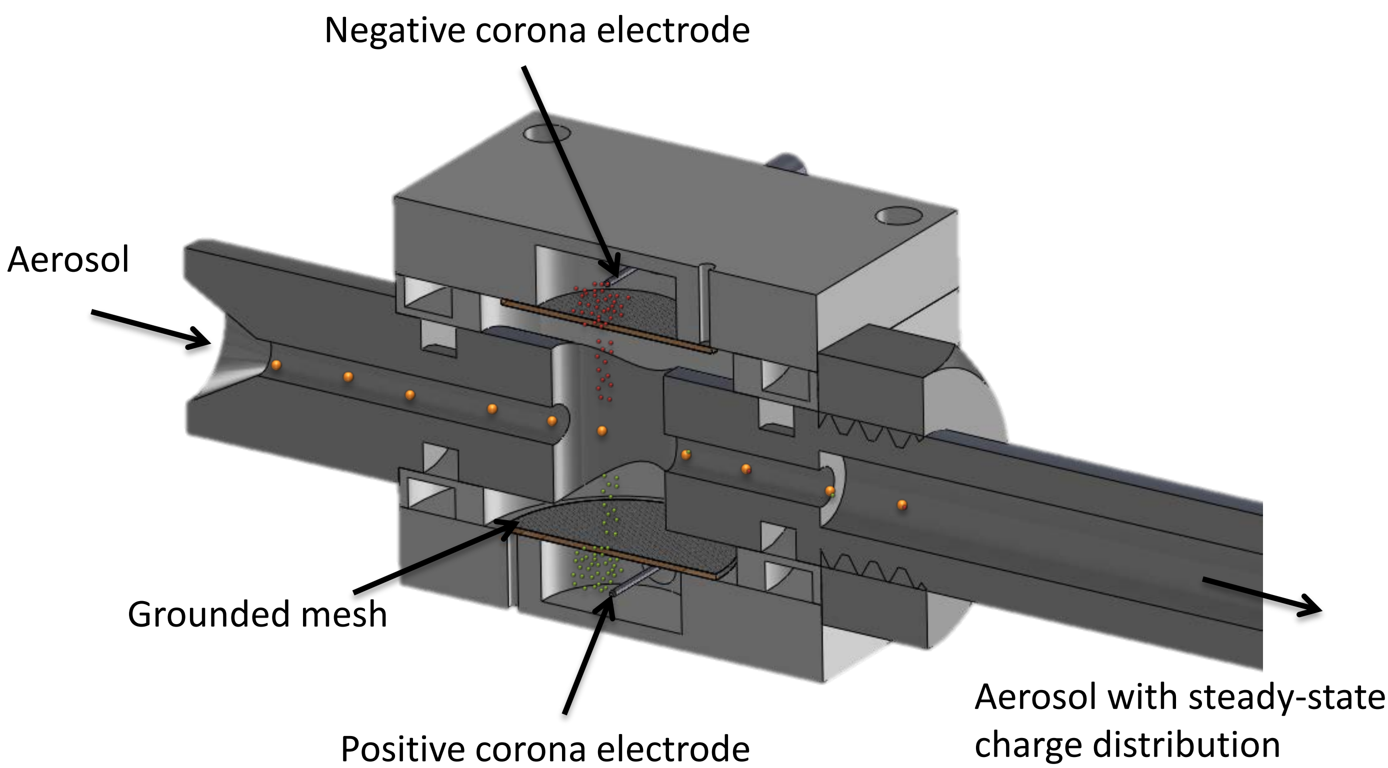

Figure S2: Cross-sectional view of the dual-corona bipolar charger

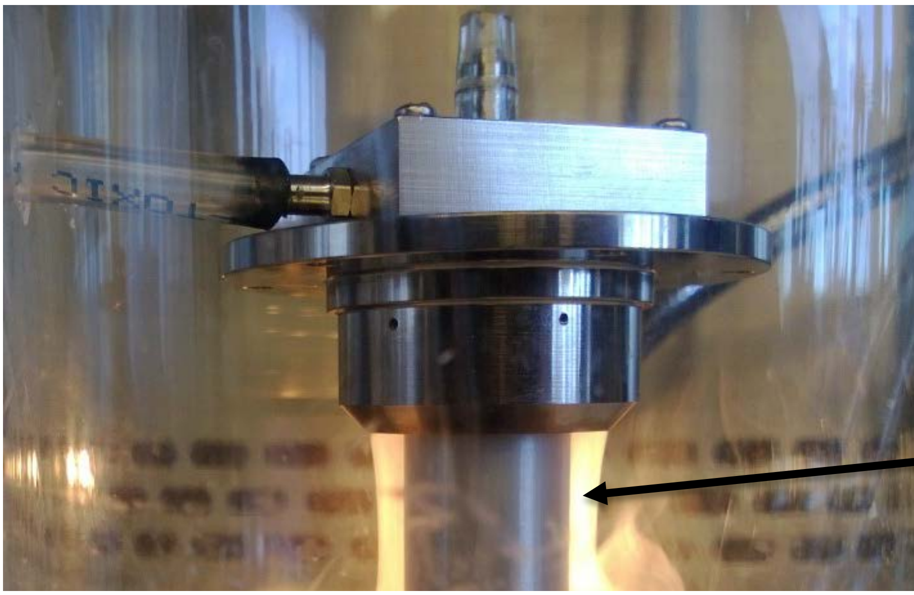

The laminar sheath flow is uniformly distributed in the azimuthal direction

Figure S3: Visualization of laminar sheath flow in mDMA

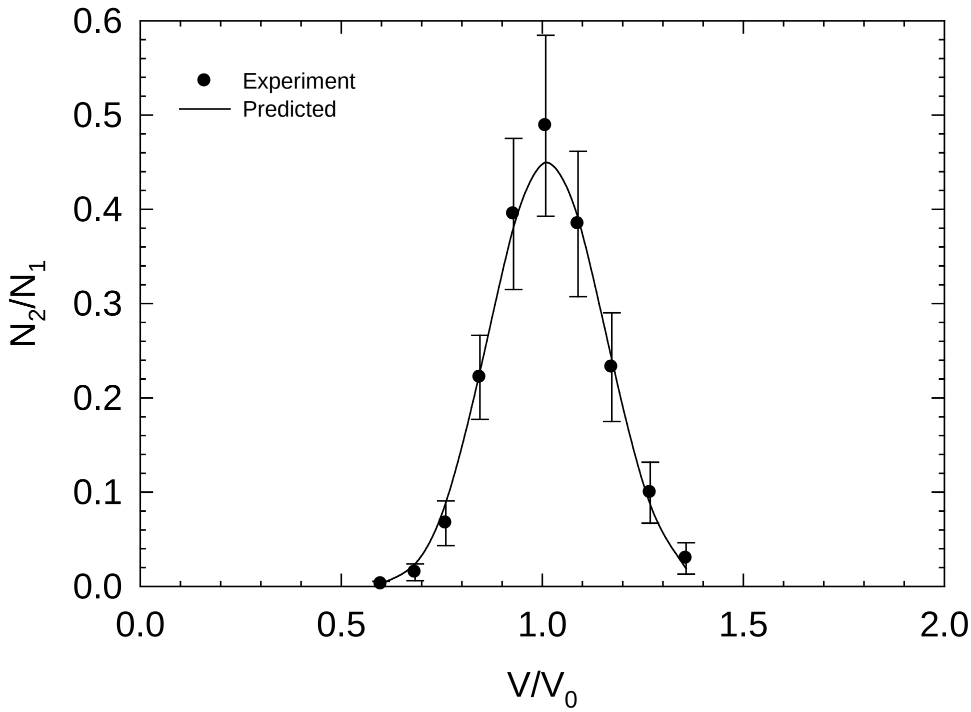

Figure S4: TDMA curves for 20 nm diameter silver particles at aerosol and sheath flow rate of 50 and 200 cm^3/min

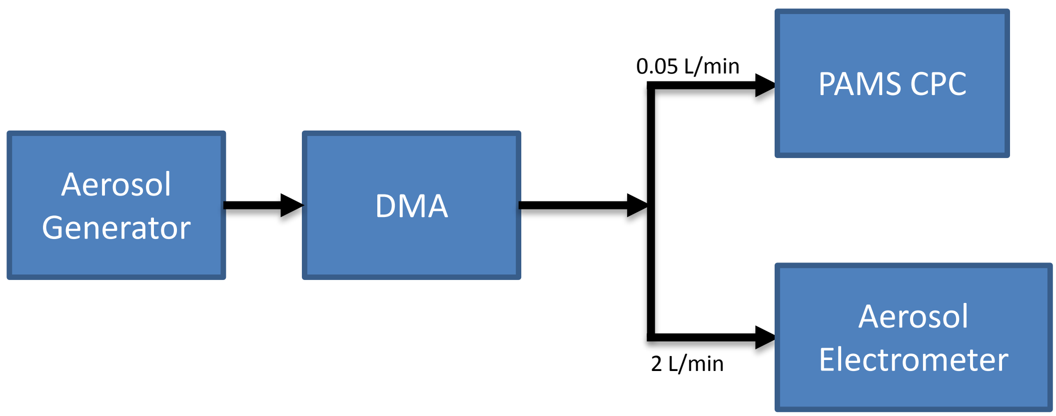

Figure S5: Experimental Setup used to calibrate the CPC. Diffusion loss in transport tubing was accounted for each instrument.

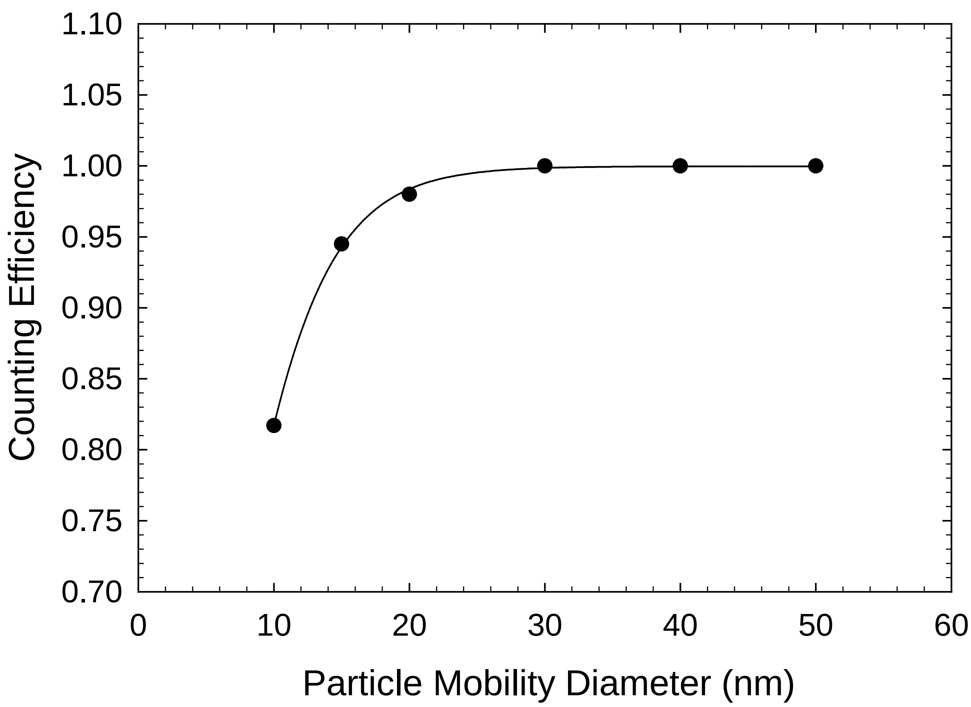

Figure S6: Activation Efficiency Curve of the CPC

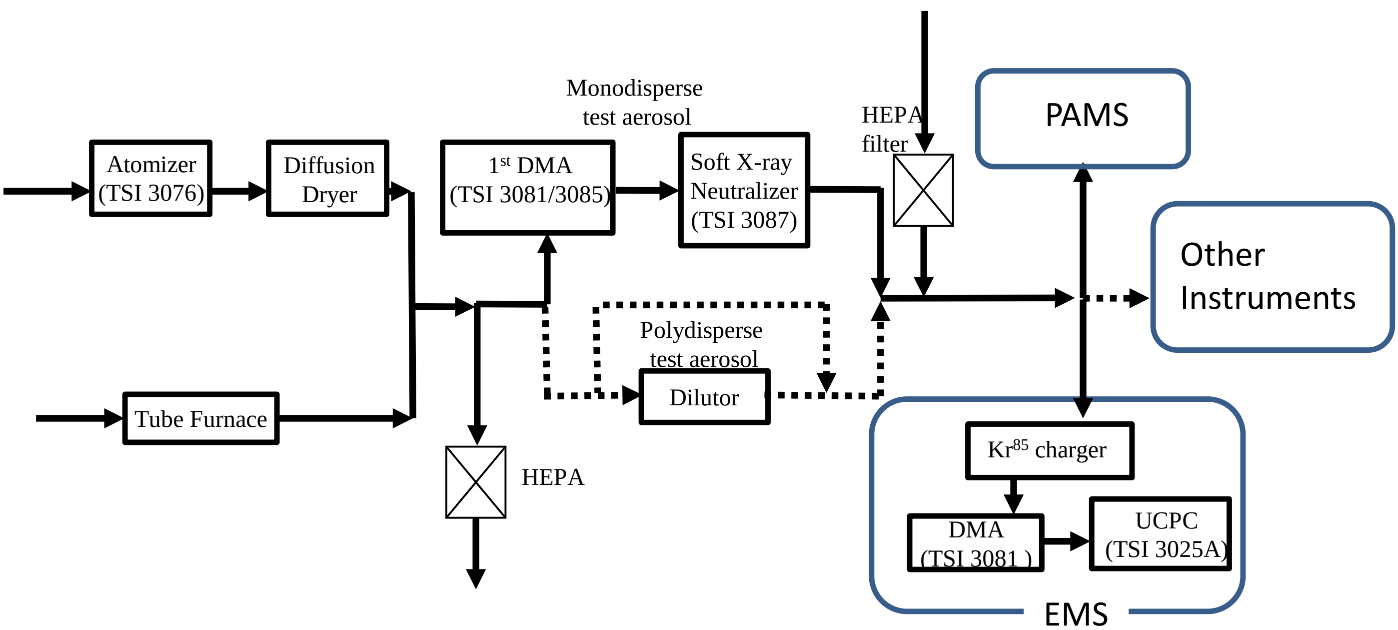

Figure S7: Schematic diagram of the Laboratory Setup used to test the performance of PAMS

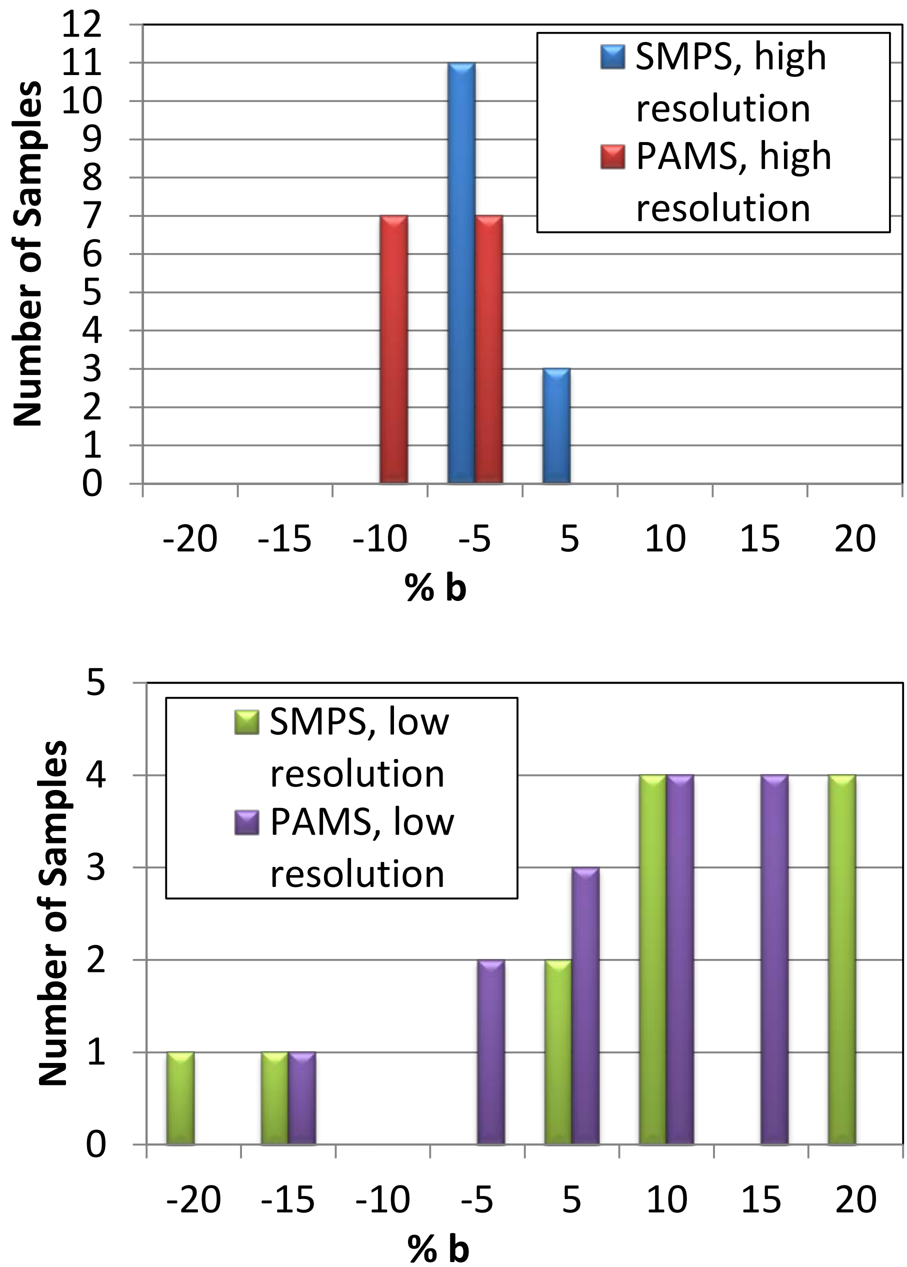

Figure S8: Bias *b* of measured d_{pg} for near-monodisperse particles at (a) high resolution and (b) low resolution

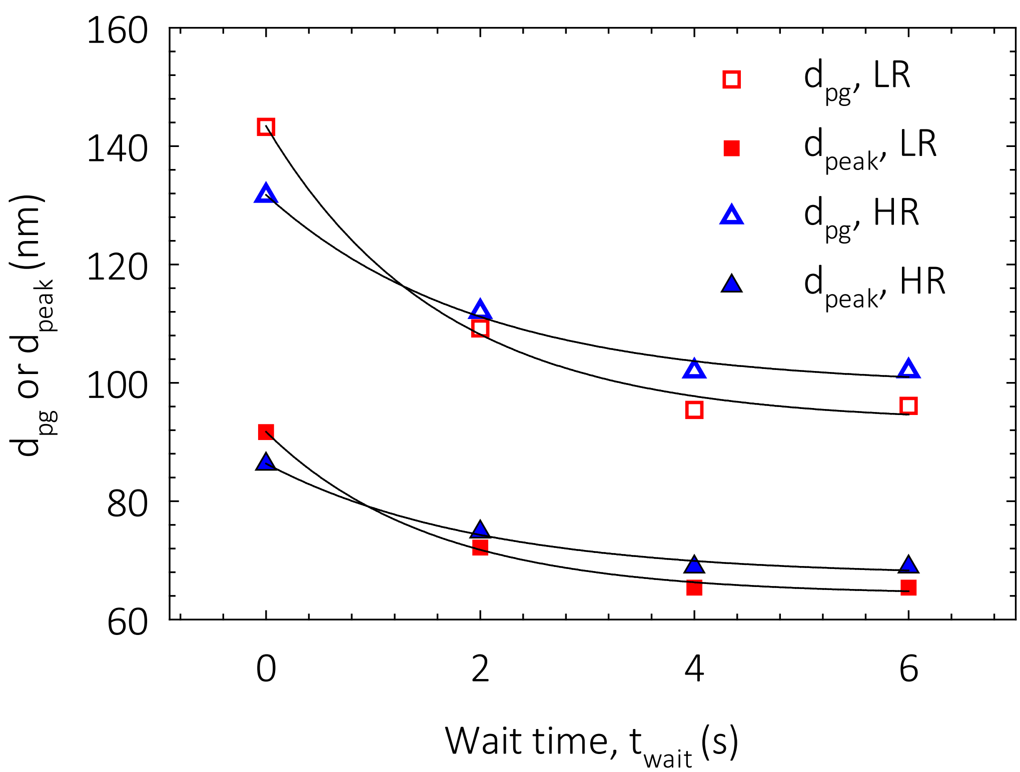

Figure S9: Variation in measured peak diameter (d_{peak}) and d_{pg} as a function of step wait time (t_{wait}) at low resolution (LR) and high resolution (HR).